Available online at www.sciencedirect.com

ScienceDirect

Mendeleev Commun., 2016, **26**, 256–258

Mendeleev Communications

Mn- and Co-substituted polyoxotungstates on MCM-41 and layered double hydroxide as catalysts in the oxidation of benzyl alcohol and cyclohexane

Wimonrat Trakarnpruk

Department of Chemistry, Faculty of Science, Chulalongkorn University, Bangkok 10330, Thailand. Fax: +662 218 7598; e-mail: wimonrat.t@chula.ac.th

DOI: 10.1016/j.mencom.2016.05.012

The Mn- and Co-substituted polyoxotungstates $[MPW_{11}O_{39}]^{5-}$ (M = Mn or Co) supported on MCM-41 or into interlayer of Mg_3Al-layered double hydroxide show catalytic activity for the solvent-free oxidation of benzyl alcohol and cyclohexane with H_2O_2.

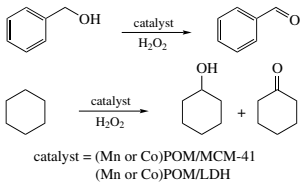

The oxidation of benzyl alcohol to benzaldehyde or cyclohexane to cyclohexanol and cyclohexanone is important in the production of perfumes and agricultural chemicals[1] or adipic acid and caprolactam,[2] respectively.

The Keggin-type polyoxotungstates $[PW_{11}MO_{39}]^{n-}$ or other polyoxometalates (POMs) have been used as catalysts for the oxidation of organic substrates due to their acidity and redox potentials.[3] Heterogenizing POM clusters on solid supports enables their effective use in liquid-phase or gas-phase reactions.[4] Mesoporous silica (MCM-41) with a high surface area, uniform and controllable pore sizes and the periodic orders of their pore packing provides a good dispersion of active species over it. $(Bu_4N)_4PW_{11}FeO_{39}$ on functionalized silica catalyzed cyclooctane oxidation using H_2O_2 in acetonitrile with higher selectivity for cyclooctanone (40%).[5] $[C_7H_7NMe_3]_7PW_{11}O_{39}$ oxidized benzyl alcohol using H_2O_2 in a solvent.[6] Layered double hydroxides (LDHs), $[M^{2+}_{1-x}M^{3+}_x(OH)_2]A^{n-}_{1-x/n}\cdot yH_2O$, are ionic lamellar solids with positively charged layers and exchangeable hydrated gallery anions.[7] CoMgAl-LDH was used for benzyl alcohol oxidation with TBHP in MeCN.[8] POMs are employed as interlayer pillaring species into LDHs using various methods.[9] Co-substituted polyoxotungstate-K10 montmorillonite[10] and $[PW_{11}MO_{39}]$-pillared Zn_2Al-LDH[11] oxidized benzyl alcohol to benzaldehyde. $K_{10}[SiW_9Co_3O_{37}]$-pillared MgAl-LDH catalyzed the oxidation of cyclohexanol with O_2,[12] while $K_5CoW_{12}O_{40}$-pillared LDH was used for benzaldehyde oxidation to benzoic acid.[13] In continuation of a work on the oxidation of cyclohexane and cyclooctane over transition metal-substituted-POM/MCM-41,[14] here the catalytic activity of Mn- and Co-substituted polyoxotungstates on MCM-41 and LDH† in the selective oxidation of benzyl alcohol and cyclohexane with H_2O_2 under solvent-free conditions is considered.

Table 1 FT-IR characteristic peaks (ν/cm^{-1}) of POMs in the catalysts.

Catalyst	P–O	W=O	W–O_b–W[b]	W–O_c–W[b]
MnPOM/MCM	1080[a]	967[a]	887	813[a]
CoPOM/MCM	1080[a]	953[a]	883	810[a]
MnPOM/LDH	1083[a]	960	890	770, 690[a]
CoPOM/LDH	1083[a]	956	887	770, 690[a]
MnPOM/LDH-adi	1079[a]	958	890	772, 688[a]
CoPOM/LDH-adi	1080[a]	955	887	772, 689[a]

[a] Masked or overlapped by bands of MCM-41 or LDH. [b] O_b is edge sharing oxygen, O_c is corner sharing oxygen.

FT-IR spectra‡ of both MnPOM/MCM and CoPOM/MCM show a tiny peak at 887 and 883 cm^{-1} (W–O–W), respectively, which reveals the existence of POM in the catalysts (Table 1). Other characteristic peaks belonging to the POM are partially overlapped with peaks from the MCM-41 (1079, 965 and 809 cm^{-1}).

A representative FT-IR spectrum of MnPOM/LDH (Figure 1) shows characteristic peaks of POM at 690–1083 cm^{-1}, which are related to the P–O, W=O, W–O_b–W and W–O_c–W vibrations. This indicates that the POM structure remained intact after ion exchange between the LDH layers. The spectrum also exhibits an OH stretching peak due to the LDH (at 3435 cm^{-1}). The FT-IR peaks of MgAl-LDH appear at 3440–3485 (OH stretching), 1620

† MCM-41 was prepared with the ratio SiO_2 : CTABr : NH_4OH : H_2O = = 1.0 : 0.12 : 8 : 114 [TEOS (26 ml) : CTABr (5 g) : NH_4OH (57 ml) : H_2O (235 g)] (CTABr is cetyltrimethylammonium bromide, TEOS is tetraethyl orthosilicate).[14] $K_5[PMW_{11}O_{39}]$[15] and $(Bu_4N)_4H[PMW_{11}O_{39}]$[16] (M = Mn or Co) were synthesized and characterized. Then, TBA-POMs (TBA is tetrabutylammonium) were supported on MCM-41 (15 wt% loading) by incipient wetness impregnation.[14] These catalysts are denoted as (Mn or Co)POM/MCM.

Mg_3Al-LDH-carbonate was synthesized by co-precipitation using $Mg(NO_3)_2$ and $Al(NO_3)_3$.[17] Its aqueous suspension was added to K-POMs (a threefold excess) at 70 °C for 5 h. The solid product was filtered, washed and dried [denoted as (Mn or Co)POM/LDH]. Another portion of Mg_3Al-LDH-carbonate was calcined to mixed oxide and rehydrated in degassed water into Mg_3Al-LDH-hydroxide in an N_2 atmosphere. This was intercalated with adipic acid.[12] Then, the resulting Mg_3Al-LDH-adipate was ion exchanged with K-POMs as above. The catalysts are denoted as (Mn or Co)POM/LDH-adi.

‡ Specific surface areas were measured using the BET method on a BELSORP-mini instrument. XRD measurements were performed on a Rigaku DMAX 2002/Ultima Plus powder X-ray diffractometer. The IR spectra were obtained on a Nicolet FT-IR Impact 410 spectrophotometer with a pressed KBr pellet. Elemental compositions were analyzed by inductively coupled plasma emission spectroscopy (ICP, Perkin Elmer model PLASMA-1000).

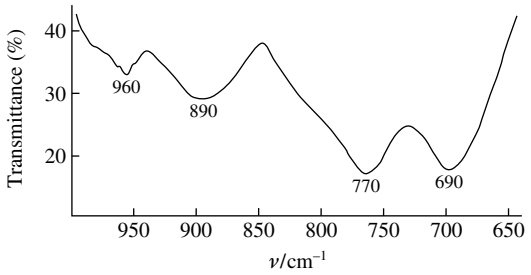

Figure 1 FT-IR spectrum of MnPOM/LDH.

(bending mode) and 670–750 cm^{-1} (metal–oxygen stretching and bending modes). Similar spectra were obtained from the MnPOM/LDH-adipate and CoPOM/LDH-adipate (Table 1).

The compositions and textural properties of the catalysts are given in Table 2. For MCM-41 supported catalysts, the found POM content (14.8–14.9%) is close to the loading value (15%). The POM loading resulted in a decrease in the BET surface area (704–715 $m^2\ g^{-1}$), pore volume (0.4 $cm^3\ g^{-1}$) and pore diameter (2.6–2.7 nm) of the catalysts. Such a decrease in these values compared to the MCM-41 implies that POM particles are confined within the channels of the MCM-41. For the LDH supported catalysts, the found Mg/Al molar ratios (2.7–2.9) are close to a ratio used in the synthesis of the Mg_3Al-LDH. The POM content in the LDH-adipate supported catalysts is higher than that in the LDH supported catalysts due to easier exchange of the labile adipate anion with POM.[12] The N_2 adsorption–desorption isotherms of all catalysts exhibit a reversible type IV one characteristic of mesoporous material.

The XRD diffraction patterns of the (Mn or Co)POM/MCM catalysts manifest a strong peak at $2\theta = 2.2°$ of (100) plane and small peaks due to higher order (110), (200) and (210) plane diffractions, indicating the formation of well-ordered mesoporous materials. Thus, the mesoporosity remains intact after the loading of POM. However, no peaks of the crystalline POM phase were observed, suggesting the high dispersion of POM in the mesoporous MCM-41 framework.

The XRD patterns of LDH and LDH-adi show peaks due to (003), (006), (102), (105) and (108) plane diffractions (Figure 2). A shift in peak positions to lower angles is observed in the case of LDH-adi. The *d*-spacing calculated from (003) plane is 0.7 and 1.3 nm in the LDH and LDH-adi, respectively. The increase

Table 2 Composition and textural properties of catalysts.

Catalyst	S_{BET}/ $m^2\ g^{-1}$	Pore volume/ $cm^3\ g^{-1}$	Pore size/nm	POM[a] (%)	P/W/M[a] in POM	Mg/Al/M[b] in catalyst
MCM-41	1040	0.8	2.9	0	–	–
MnPOM/ MCM	704	0.4	2.6	14.9	1/11/0.98	–
CoPOM/ MCM	715	0.4	2.7	14.8	1/10.9/0.97	–
LDH	118	0.4	8.9	–	–	2.9/1/0
MnPOM/ LDH	91	0.3	7.0	–	1/10.9/0.97	2.9/1/0.13
CoPOM/ LDH	88	0.3	6.9	–	1/10.9/0.97	2.8/1/0.11
LDH-adi	125	0.5	9.4	–	–	2.8/1/0
MnPOM/ LDH-adi	104	0.4	9.2	–	1/10.9/0.98	2.7/1/0.46
CoPOM/ LDH-adi	105	0.4	9.2	–	1/10.8/0.98	2.8/1/0.45

[a] By ICP, POM loading in MCM-41 is 15 wt%. [b] By ICP, Mg/Al loading molar ratio in LDH and POM/LDH loading weight ratio are equal to 3. M = Mn or Co.

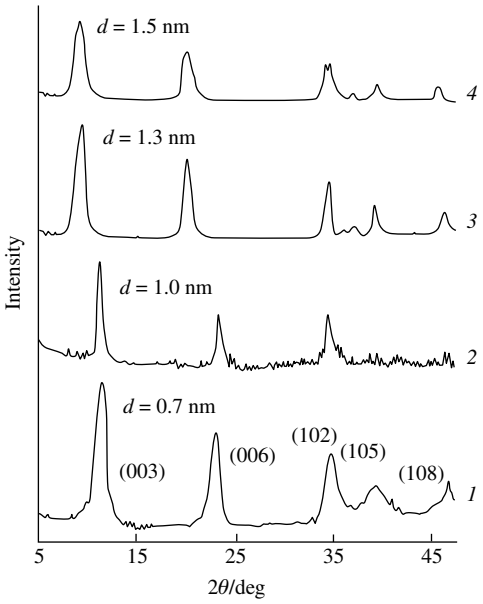

Figure 2 XRD patterns of (*1*) LDH, (*2*) MnPOM/LDH, (*3*) LDH-adi and (*4*) MnPOM/LDH-adi.

of the *d*-spacing in the LDH-adi indicates adipate intercalation in the interlayer of LDH. After loading with POM, the peak position was shifted, corresponding to an increase in the *d*-spacing in the (Mn or Co)POM/LDH (1.0 nm) and (Mn or Co)POM/LDH-adi catalysts (1.5 nm). The peak intensities from both catalysts also decrease, reflecting a lower degree of crystallinity. The broadening of peaks can also be due to a smaller crystal size.

The results of the oxidation of benzyl alcohol[§] are given in Table 3. The catalytic activity of CoPOM/MCM is slightly higher than that of MnPOM/MCM. The conversion grows with reaction time but selectivity for benzaldehyde diminishes (increases for benzoic acid). The enhancement of catalytic activity by supporting

Table 3 Oxidation of benzyl alcohol (10 ml, 5 wt% catalyst, H_2O_2/alcohol molar ratio of 3:1, 90 °C).

Catalyst	*t*/h	Conversion (%)	Selectivity for benzaldehyde (%)
–	5	2	70
MnPOM/MCM	5	67	75
	8	76	69
CoPOM/MCM	5	70	71
	8	78	67
TBA-MnPOM[a]	5	49	75
TBA-CoPOM[a]	5	52	70
TBA-MnPOM[b]	2.5	35	Not determined
TBA-CoPOM[b]	2.5	13	Not determined
LDH	5	3	91
MnPOM/LDH	5	45	97
CoPOM/LDH	5	37	96
LDH-adi	5	4	90
MnPOM/LDH-adi	5	66	100
CoPOM/LDH-adi	5	69	99

[a] H_2O_2/alcohol molar ratio of 2:1. [b] H_2O_2/alcohol molar ratio of 5:1, in H_2O, 100 °C.[11]

§ *Oxidation reaction*. Substrate (benzyl alcohol or cyclohexane), catalyst and aqueous H_2O_2 (30%) were inserted into a 60 ml Parr reactor. The reactor was heated to a desired temperature and the mixture was stirred. The catalyst was separated, and the products were extracted with diethyl ether, dried and analyzed by GC [chromatograph, Varian CP-3800 GC; column, CP-Sil (30 m × 0.25 mm)].

Table 4 Oxidation of cyclohexane (10 ml, 5 wt% catalyst, 80 °C, 8 h).

Catalyst	H_2O_2/cyclohexane molar ratio	Conversion (%)	Selectivity to cyclohexanone (%)
MCM	4:1	0	0
MnPOM/MCM	4:1	12	76
CoPOM/MCM	4:1	15	73
TBA-MnPOM[a]	2:1	4	45
TBA-CoPOM[a]	2:1	5	40
LDH-adi	3:1	0	0
MnPOM/LDH-adi	3:1	19	73
CoPOM/LDH-adi	3:1	18	72

[a] Cyclohexane, 18.5 mmol; catalyst, 0.04 mmol; MeCN, 10 ml; 12 h.[14]

POM on the MCM-41 is believed to be due to the adsorption in high surface area of the support and the vicinity of the POM active site and oxidant within the mesopores of the support. For comparison, $Cs_5PCoMo_{11}O_{39}$ was reported to oxidize benzyl alcohol more effectively (56% conversion) than $Cs_5PMnMo_{11}O_{39}$ (38% conversion).[1] Reduction potentials of $K_5PCoW_{11}O_{39}$ and $K_5PMnW_{11}O_{39}$ were found at –0.506 and –0.497 V, respectively.[15]

The activities of the POM loaded-LDH and POM loaded-LDH-adipate catalysts are higher than that of the POM-free catalysts. It was reported that activities of clay-supported catalyst are due to easier reduction of metal ion *via* interaction of POM anion with the clay surface.[10] The higher selectivity for benzaldehyde from the LDH-supported catalysts compared to the unsupported catalysts is caused by the basic sites of catalysts.[8]

The results of the oxidation of cyclohexane[8] are summarized in Table 4. The pure supports do not reveal activity under the reaction conditions. The CoPOM/MCM provides higher cyclohexane conversion than the MnPOM/MCM. The supported catalysts show higher selectivity for cyclohexanone than the homogeneous system. MCM-41 matrices might modify the reaction. The produced cyclohexanol is adsorbed in the mesopores of the MCM-41 and then further oxidized to cyclohexanone.[14] A similar result was previously reported for the oxidation of alkane over vanadium polyoxometalate/MCM-41 catalysts.[18]

Based on the results of a usability test, the catalysts can be repeatedly used four times without remarkable loss of activity and selectivity.

References

1 S. Pathan and A. Patel, *Appl. Catal., A*, 2013, **459**, 59.
2 A. K. Suresh, M. M. Sharma and T. Sridhar, *Ind. Eng. Chem. Res.*, 2000, **39**, 3958.
3 (*a*) M. M. Q. Simões, I. C. M. S. Santos, M. S. S. Balula, J. A. F. Gamelas, A. M. V. Cavaleiro, M. G. P. M. S. Neves and J. A. S. Cavaleiro, *Catal. Today*, 2004, **91–92**, 211; (*b*) N. Mizuno, J.-S. Min and A. Taguchi, *Chem. Mater*., 2004, **16**, 2819; (*c*) I. C. M. S. Santos, J. A. F. Gamelas, M. S. S. Balula, M. M. Q. Simões, M. G. P. M. S. Neves, J. A. S. Cavaleiro and A. M. V. Cavaleiro, *J. Mol. Catal., A: Chem*., 2007, **262**, 41.
4 (*a*) M. R. Farsani and B. Yadollahi, *J. Mol. Catal. A: Chem.*, 2014, **392**, 8; (*b*) W. Trakarnpruk, *Mendeleev Commun.*, 2014, **24**, 167.
5 A. C. Estrada, I. C. M. S. Santos, M. M. Q. Simões, M. G. P. M. S. Neves, J. A. S. Cavaleiro and A. M. V. Cavaleiro, *Appl. Catal., A*, 2011, **392**, 28.
6 Z. Weng, J. Wang and X. Jian, *Catal. Commun.*, 2008, **9**, 1688.
7 V. Rives and M. A. Ulibarri, *Coord. Chem. Rev*., 1999, **181**, 61.
8 W. Zhou, J. Liu, J. Pan, F. Sun, M. He and Q. Chen, *Catal. Commun.*, 2015, **69**, 1.
9 E. Narita, P. D. Kaviratna and T. J. Pinnavaia, *J. Chem. Soc., Chem. Commun.*, 1993, 60.
10 G. B. B. Varadwaj, S. Rana and K. Parida, *Chem. Eng. J*., 2013, **215–216**, 849.
11 S. Hasannia and B. Yadollahi, *Polyhedron*, 2015, **99**, 260.
12 S. K. Jana, Y. Kubota and T. Tatsumi, *J. Catal*., 2008, **255**, 40.
13 X. Wei, Y. Fu, L. Xu, F. Li, B. Bi and X. Liu, *J. Solid State Chem*., 2008, **181**, 1292.
14 J. Jatupisarnpong and W. Trakarnpruk, *Mendeleev Commun*., 2012, **22**, 152.
15 J. H. Choi, J. K. Kim, D. R. Park, T. H. Kang, J. H. Song and I. K. Song, *J. Mol. Catal. A: Chem.*, 2013, **371**, 111.
16 M. M. Q. Simões, C. M. M. Conceição, J. A. F. Gamelas, P. M. D. N. Domingues, A. M. V. Cavaleiro, J. A. S. Cavaleiro, A. J. V. Ferrer-Correia and R. A. W. Johnstone, *J. Mol. Catal. A: Chem.*, 1999, **144**, 461.
17 W. Trakarnpruk and W. Kanjina, *Mendeleev Commun.*, 2012, **22**, 275.
18 V. Tangestaninejad, M. Mirkhani, V. Moghadam, M. Mohammadpoor-Baltork, E. Shams and H. Salavati, *Ultrason. Sonochem.*, 2008, **15**, 438.

Received: 26th October 2015; Com. 15/4760